

Children's Mercy Kansas City

## SHARE @ Children's Mercy

---

Manuscripts, Articles, Book Chapters and Other Papers

---

8-1-2023

### **Cation leak through the ATP1A3 pump causes spasticity and intellectual disability.**

Daniel G. Calame

Cristina Moreno Vadillo

Seth Berger

Timothy Lotze

Marwan Shinawi

*See next page for additional authors*

|   |
|---|
| Let us know how access to this publication benefits you |
|---|

Follow this and additional works at: <https://scholarlyexchange.childrensmercy.org/papers>

---


---

**Creator(s)**

Daniel G. Calame, Cristina Moreno Vadillo, Seth Berger, Timothy Lotze, Marwan Shinawi, Javaher Poupak, Corina Heller, Julie Cohen, Richard Person, Aida Telegrafi, Chalongchai Phitsanu Wong, Kaylene Fiala, Isabelle Thiffault, Florencia Del Viso, Dihong Zhou, Emily A. Fleming, Tomi Pastinen, Ali Fatemi, Sruthi Thomas, Samuel I. Pascual, Rosa J. Torres, Carmen Prior, Clara Gómez-González, Saskia Biskup, James R. Lupski, Dragan Maric, Miguel Holmgren, Debra Regier, and Sho T. Yano



# Cation leak through the ATP1A3 pump causes spasticity and intellectual disability

Daniel G. Calame,<sup>1,2,3</sup> Cristina Moreno Vadillo,<sup>4</sup> Seth Berger,<sup>5</sup> Timothy Lotze,<sup>1,3</sup> Marwan Shinawi,<sup>6</sup> Javaher Poupak,<sup>7</sup> Corina Heller,<sup>8,9</sup> Julie Cohen,<sup>10,11</sup> Richard Person,<sup>12</sup> Aida Telegrafi,<sup>12</sup> Chalongchai Phitsanuwoong,<sup>13</sup> Kaylene Fiala,<sup>13</sup> Isabelle Thiffault,<sup>14,15,16</sup> Florencia Del Viso,<sup>14,16</sup> Dihong Zhou,<sup>15,17</sup> Emily A. Fleming,<sup>17</sup> Tomi Pastinen,<sup>14,15</sup> Ali Fatemi,<sup>10,11,18</sup> Sruthi Thomas,<sup>19</sup> Samuel I. Pascual,<sup>20</sup> Rosa J. Torres,<sup>21,22</sup> Carmen Prior,<sup>23</sup> Clara Gómez-González,<sup>23</sup> Saskia Biskup,<sup>8,9</sup> James R. Lupski,<sup>2,3,24,25</sup> Dragan Maric,<sup>26</sup> Miguel Holmgren,<sup>4</sup> Debra Regier<sup>5</sup> and  Sho T. Yano<sup>27</sup>

ATP1A3 encodes the  $\alpha 3$  subunit of the sodium-potassium ATPase, one of two isoforms responsible for powering electrochemical gradients in neurons. Heterozygous pathogenic ATP1A3 variants produce several distinct neurological syndromes, yet the molecular basis for phenotypic variability is unclear.

We report a novel recurrent variant, ATP1A3(NM\_152296.5):c.2324C>T; p.(Pro775Leu), in nine individuals associated with the primary clinical features of progressive or non-progressive spasticity and developmental delay/intellectual disability. No patients fulfil diagnostic criteria for ATP1A3-associated syndromes, including alternating hemiplegia of childhood, rapid-onset dystonia-parkinsonism or cerebellar ataxia-areflexia-pes cavus-optic atrophy-sensorineural hearing loss (CAPOS), and none were suspected of having an ATP1A3-related disorder. Uniquely among known ATP1A3 variants, P775L causes leakage of sodium ions and protons into the cell, associated with impaired sodium binding/occlusion kinetics favouring states with fewer bound ions.

These phenotypic and electrophysiologic studies demonstrate that ATP1A3:c.2324C>T; p.(Pro775Leu) results in mild ATP1A3-related phenotypes resembling complex hereditary spastic paraplegia or idiopathic spastic cerebral palsy. Cation leak provides a molecular explanation for this genotype-phenotype correlation, adding another mechanism to further explain phenotypic variability and highlighting the importance of biophysical properties beyond ion transport rate in ion transport diseases.

- 1 Section of Pediatric Neurology and Developmental Neuroscience, Department of Pediatrics, Baylor College of Medicine, Houston, TX 77030, USA
- 2 Department of Molecular and Human Genetics, Baylor College of Medicine, Houston, TX 77030, USA
- 3 Texas Children's Hospital, Houston, TX 77030, USA
- 4 National Institute of Neurological Disorders and Stroke, National Institutes of Health, Bethesda, MD 20892, USA
- 5 Children's National Rare Disease Institute, Children's National Hospital, Washington, DC 20012, USA
- 6 Department of Pediatrics, Division of Genetics and Genomic Medicine, Washington University School of Medicine, St. Louis, MO 63110, USA
- 7 Zentrum Für Labormedizin, St. Gallen 9001, Switzerland
- 8 Praxis Für Humangenetik Tübingen, Tuebingen 72076, Germany
- 9 CeGaT GmbH, Tuebingen 72076, Germany
- 10 Department of Neurology and Developmental Medicine, Kennedy Krieger Institute, Baltimore, MD 21205, USA
- 11 Department of Neurology, Johns Hopkins University School of Medicine, Baltimore, MD 21287, USA
- 12 GeneDX, Gaithersburg, MD 20879, USA

- 13 Section of Pediatric Neurology, Department of Pediatrics, Comer Children's Hospital, University of Chicago, Chicago, IL 60637, USA
- 14 Genomic Medicine Center, Children's Mercy Research Institute, Kansas City, MO 64108, USA
- 15 School of Medicine, University of Missouri Kansas City, Kansas City, MO 64108, USA
- 16 Department of Pathology and Laboratory Medicine, Children's Mercy Hospital, Kansas City, MO 64108, USA
- 17 Department of Genetics, Children's Mercy Hospital, Kansas City, MO 64108, USA
- 18 Department of Pediatrics, Johns Hopkins University School of Medicine, Baltimore, MD 21287, USA
- 19 Departments of Physical Medicine & Rehabilitation and Neurosurgery, Baylor College of Medicine, Houston, TX 77030, USA
- 20 Department of Pediatric Neurology, La Paz University Hospital, Madrid, Spain
- 21 La Paz University Hospital Health Research Institute (FIBHULP), IdiPaz, Madrid, Spain
- 22 Center for Biomedical Network Research on Rare Diseases (CIBERER), Instituto de Salud Carlos III, 20829 Madrid, Spain
- 23 Department of Genetics, Genetic Service, La Paz University Hospital, Madrid, Spain
- 24 Human Genome Sequencing Center, Baylor College of Medicine, Houston, TX 77030, USA
- 25 Department of Pediatrics, Baylor College of Medicine, Houston, TX 77030, USA
- 26 Flow and Imaging Cytometry Core Facility, National Institute of Neurological Disorders and Stroke, National Institutes of Health, Bethesda, MD 20892, USA
- 27 National Human Genome Research Institute, National Institutes of Health, Bethesda, MD 20892, USA

Correspondence to: Sho Yano  
 National Human Genome Research Institute  
 National Institutes of Health  
 35 Convent Drive, 3F123, Bethesda, MD 20892, USA  
 E-mail: sho.yano@nih.gov

**Keywords:** ATP1A3; sodium-potassium ATPase; neurodevelopmental disorders; spastic paraparesis; spasticity

## Introduction

Sodium-potassium ATPase ( $\text{Na}^+/\text{K}^+$ -ATPase) generates transmembrane gradients of sodium ( $\text{Na}^+$ ) and potassium ( $\text{K}^+$ ) that power neuronal activity.<sup>1</sup> Each enzymatic cycle pumps 3  $\text{Na}^+$  out of the cell in exchange for 2  $\text{K}^+$  at the cost of 1 ATP. The core enzyme is an  $\alpha/\beta$  heterodimer; the catalytic  $\alpha$  subunit contributes all three ion binding sites and the ATPase domain. Two  $\alpha$  isoforms,  $\alpha 1$  and  $\alpha 3$ , predominate among neurons in the brain.<sup>2</sup>

Heterozygous pathogenic variants in ATP1A3, encoding  $\alpha 3$ , cause a wide range of neurological diseases. Asymmetric paroxysmal movement disorder phenotypes such as alternating hemiplegia of childhood (AHC) and rapid-onset dystonia-parkinsonism (RDP) are the best described.<sup>3–5</sup> They occur with additional features like epilepsy and intellectual disability in AHC. Other distinct phenotypes include CAPOS (cerebellar ataxia, areflexia, pes cavus, optic atrophy, sensorineural hearing loss) due to the recurrent p.(Glu818Lys) variant, early-infantile epileptic encephalopathy, slowly progressive cerebellar ataxia and polymicrogyria.<sup>6–10</sup>

The mechanism by which ATP1A3 variants produce such a wide variety of neurological syndromes is unknown. ATP1A3 pathogenic variants impair ion transport, yet the rate of transport does not correlate with disease severity in AHC/RDP variants.<sup>11</sup> The existence of genotype-phenotype correlations suggests other factors related to ATP1A3 genotype influence what set of symptoms a patient will experience.

Here, we identify a novel recurrent ATP1A3 variant, c.2324C>T; p.(Pro775Leu), in nine patients with progressive or non-progressive spasticity and developmental delay/intellectual disability (DD/ID). None of the patients meet diagnostic criteria for ATP1A3-related disorders or were suspected of having an ATP1A3-related disorder

prior to genetic testing. This mild manifestation of ATP1A3 disease results from P775L causing leakage of  $\text{Na}^+$  and protons ( $\text{H}^+$ ) into the cell, associated with disruption of extracellular  $\text{Na}^+$  binding/occlusion. The association of this strong genotype-phenotype correlation with a new molecular mechanism in ATP1A3-associated disease provides another mechanism to further explain phenotypic variability and highlights the importance of biophysical properties beyond ion transport rate in ion transport diseases.

## Materials and methods

### Patients and genetic testing

All patients or guardians provided written informed consent for study participation and publication under Baylor College of Medicine (BCM) Institutional Review Board (IRB) protocol H-29697 or other collaborative local IRBs. Patients underwent clinical trio (3), duo (4) or singleton (1) exome sequencing (ES) or next generation sequencing panel-based testing (1) at Baylor Genetics, Center for Human Genetics Tuebingen, University of Chicago Genetic Services Laboratories, Children's Mercy Hospital, GeneDx or La Paz University Hospital.

### Ouabain complementation assay

HEK293 T cells were transfected with ouabain-resistant ATP1A3 expression vectors for 2 days then transferred to ouabain-containing medium (Supplementary material, 'Methods' section).<sup>3</sup> Since not all ouabain-killed cells immediately lost membrane integrity (Supplementary Fig. 1), we measured the total number of cells remaining after 2 days.

## Electrophysiology

*Xenopus* oocytes were co-injected with human ouabain-resistant ATP1A3 and ATP1B1 coding RNAs. This functional complex will be denoted ‘wild-type’ for simplicity. Na<sup>+</sup>/K<sup>+</sup>-ATPase-specific currents were measured by two-electrode voltage clamp after 2–4 days or cut-open vaseline gap voltage clamp after 4–6 days (Supplementary material, ‘Methods’ section).

## Statistical analysis

Statistical analysis was done in GraphPad Prism 9. Survival and current means were compared to wild-type using Dunnett’s test. Reversal potentials presented are means ± standard deviations. All error bars represent 95% confidence intervals (CI).

## Results

### Spasticity and developmental abnormalities in unrelated probands with ATP1A3 p.(Pro775Leu) variant

The index patient was a 17-year-old female with spastic paraplegia and DD/ID (Fig. 1A, Family 1). Through duo ES a heterozygous ATP1A3 variant NM\_152296.5:c.2324C>T; p.(Pro775Leu) was identified in the proband but not her unaffected mother. The variant is absent from gnomAD v2.1.1 [141 456 ES and genome sequences (GS)] and the BCM Genomics Research Elucidates the Genetics of Rare disease (GREGOR) database (12 281 ES and GS). The position is highly conserved (Supplementary Fig. 2), lies in the fifth transmembrane domain of ATP1A3 (Fig. 1B),<sup>12,13</sup> and its change to Leu is predicted to be damaging by *in silico* algorithms (REVEL 0.7659, CADD 26.0).<sup>14,15</sup> The variant was classified as a variant of uncertain significance (VUS) by Baylor Genetics diagnostic laboratory in 2016.

In light of the variant’s classification as a VUS and the lack of a phenotypic match with known ATP1A3-related syndromes, we searched for additional patients with ATP1A3:c.2324C>T; p.(Pro775Leu) through diagnostic laboratory queries and personal communications with colleagues. These efforts uncovered eight additional individuals with spasticity and DD/ID (Fig. 1A). The variant occurred *de novo* in Families 3, 7, 8 and 9, whereas *de novo* status could not be ascertained in all other families due to lack of parental samples. None of these families had parental history of spasticity, DD/ID or other neurologic disorders suggestive of mildly affected parents. As ATP1A3(NM\_152296.5):c.2324C>T; p.(Pro775Leu) corresponds to ATP1A3(NM\_001256214.2):c.2363C>T; p.(Pro788Leu), it has possibly been reported in one father-son pair with atypical RDP/CAPOS with symmetric leg dystonia, decreased reflexes and positive Babinski sign; however, a RefSeq or Ensembl transcript was not provided.<sup>16</sup>

The clinical features associated with ATP1A3:c.2324C>T; p.(Pro775Leu) are shown in Fig. 1C and the Supplementary material. All patients exhibited spasticity and DD/ID. Most had spastic diplegia beginning in childhood. Spasticity was progressive in five patients and non-progressive in the remainder. Other common features include axial hypotonia, hyperreflexia, attention deficit hyperactivity disorder, obesity, bowel and bladder incontinence and seizures. Two patients had episodic disease progression. In Family 1, the proband had sudden gait deterioration, a stepwise loss of ambulatory ability triggered by sickle cell pain crises. In Family 2, the proband had severe developmental regression after an episode of prolonged rigidity with cyanosis during a febrile

illness at 16 months of age. Two patients had hemiplegic episodes. Hemiplegic episodes were infrequent in Family 3 and began after 18 months of age. In Family 6, they consisted of hemiplegic migraines with onset at 9 years of age. Brain MRI was normal in eight of nine individuals (Fig. 1C, Supplementary Fig. 3 and Supplementary material) and did not show changes over time in those with serial imaging (Supplementary material). Brain imaging of proband in Family 2 after his developmental regression showed severe diffuse encephalomalacia consistent with a hypoxic-ischaemic event (Supplementary Fig. 3).

No patient’s features met diagnostic criteria for AHC, RDP or CAPOS, or resembled other rare ATP1A3 syndromes.<sup>9,10,17,18</sup> Thus, ATP1A3:c.2324C>T; p.(Pro775Leu) results in mild ATP1A3 phenotypes resembling complex hereditary spastic paraplegia (HSP) and spastic cerebral palsy (CP).

### P775L reverses the direction of charge transport through $\alpha 3$ -Na<sup>+</sup>/K<sup>+</sup>-ATPase

To investigate the hypothesized pathogenicity of ATP1A3:c.2324C>T; p.(Pro775Leu) and understand its unusual phenotype association, we examined its impact on  $\alpha 3$ -Na<sup>+</sup>/K<sup>+</sup>-ATPase activity. P775L caused loss-of-function in the ouabain complementation assay (Fig. 2A), which measured the ability of transfected ATP1A3 to rescue cell survival when endogenous Na<sup>+</sup>/K<sup>+</sup>-ATPases were blocked by a specific inhibitor, ouabain. The P775L variant ATP1A3 rescued significantly less survival than the wild-type ( $P = 0.006$ ). The effect of P775L was similar to that of p.Asp801Asn (D801N), the most common pathogenic variant in AHC (Fig. 2A).

Next, we expressed human ATP1A3-containing  $\alpha 3$ -Na<sup>+</sup>/K<sup>+</sup>-ATPase in *Xenopus* oocytes for two-electrode voltage clamp measurements of ion transport. When oocytes were loaded with intracellular Na<sup>+</sup> (Na<sub>i</sub><sup>+</sup>), normal ion transport by wild-type  $\alpha 3$ -Na<sup>+</sup>/K<sup>+</sup>-ATPase was readily measurable as positive, ouabain-sensitive, steady-state ‘pump currents’ elicited by extracellular K<sup>+</sup> (K<sub>o</sub><sup>+</sup>) (Supplementary Fig. 4). Figure 2B displays these currents at 0 mV, while Fig. 2C shows the average current from 10 oocytes as between –100 and +30 mV. Wild-type enzymes also occasionally import protons (H<sup>+</sup>) during normal Na<sup>+</sup>/K<sup>+</sup> transport cycles; however, this ‘H<sup>+</sup> leak current’ is very small under physiological conditions (1 H<sup>+</sup> per ~25–30 transport cycles) and inhibited by extracellular Na<sup>+</sup> (Na<sub>o</sub><sup>+</sup>).<sup>19</sup> Accordingly, minimal current was generated in the absence of K<sub>o</sub><sup>+</sup> (Fig. 2D). In contrast, oocytes expressing P775L  $\alpha 3$ -Na<sup>+</sup>/K<sup>+</sup>-ATPase lacked positive currents, indicating loss of normal ion transport (Fig. 2B and C and Supplementary Fig. 4). At 0 mV, this effect was significant against wild-type ( $P < 0.0001$ ) (Fig. 2B). It was similar to that of D801N across all tested voltages (Fig. 2C).

Surprisingly, oocytes expressing P775L  $\alpha 3$ -Na<sup>+</sup>/K<sup>+</sup> ATPase exhibited abnormal negative ‘leak’ currents at negative potentials which were absent with wild-type and D801N, representing ionic currents in the opposite direction from normal transport (Fig. 2C). P775L leak occurred in both the presence and absence of K<sub>o</sub><sup>+</sup> (Fig. 2D) with a reversal potential near 0 mV, suggesting that either Na<sup>+</sup> or H<sup>+</sup> was the main ion species involved.

To verify that P775L  $\alpha 3$ -Na<sup>+</sup>/K<sup>+</sup>-ATPases reached the cell membrane, we confirmed that they produce extracellular Na<sup>+</sup>-mediated transient currents representing binding/unbinding of Na<sub>o</sub><sup>+</sup> in response to voltage pulses (Supplementary Fig. 5). Time-integrating these transient currents yielded charge bound, Q, which was moderately decreased compared to wild-type (Fig. 2E). Normally, Q follows a Boltzmann sigmoidal function of

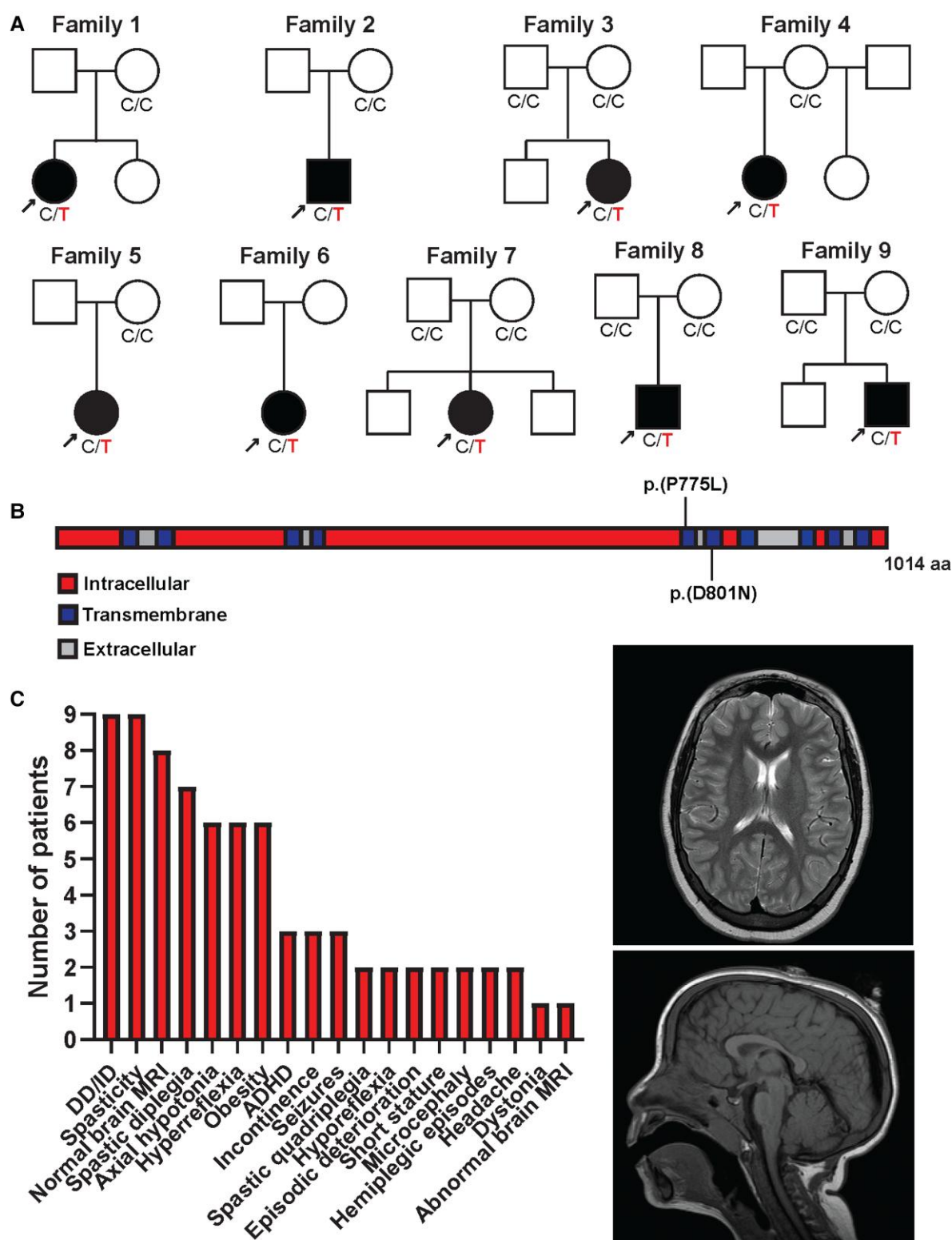


**Figure 1** Clinical and molecular synopsis of ATP1A3:c.2324C>T; p.(Pro775Leu). (A) Pedigrees of families with ATP1A3:c.2324C>T; p.(Pro775Leu). Affected individuals are indicated by filled circles and squares and with arrows. Genotype at the locus is indicated below pedigree symbols if available; variant alleles are indicated in red. (B) Protein domain structure of ATP1A3. Intracellular domains are shown in red, transmembrane domains in blue, and extracellular domains in grey. (C) Phenotypic traits associated with ATP1A3:c.2324C>T; p.(Pro775Leu) are shown in order of frequency. Representative T<sub>2</sub>-weighted axial brain magnetic resonance imaging (top) and T<sub>1</sub>-weighted sagittal brain MRI (bottom) from proband in Family 1 showing normal supratentorial brain structure, cerebellum and brainstem.

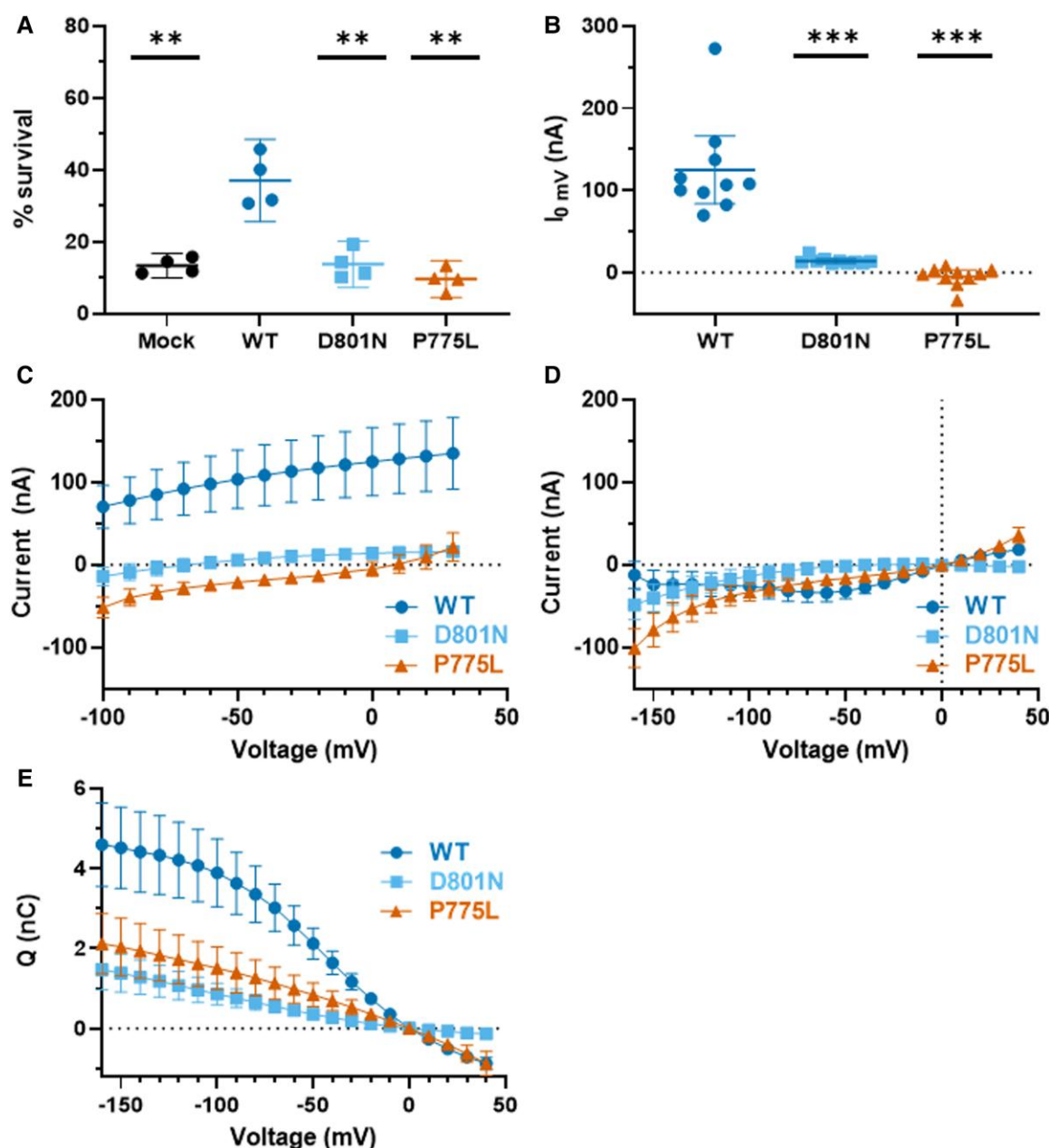


**Figure 2** P775L eliminates normal  $\alpha 3$ -Na<sup>+</sup>/K<sup>+</sup>-ATPase function and introduces inward current leak. (A) P775L shows loss-of-function in an ouabain complementation assay. HEK293 T cells were either mock-transfected (Mock) or transfected with ouabain-resistant ATP1A3 expression constructs with no additional variants (WT) or the D801N and P775L variants as shown. Two days after transfection, half of the cells were transferred to medium with or without 10  $\mu$ M ouabain for another 2 days. The percentage of surviving cells in ouabain compared to the same sample without ouabain is shown. Each point represents one replicate with error bars at 95% CI. \*\* $P < 0.01$  versus wild-type (WT). (B) P775L eliminates normal ion transport currents. Na<sup>+</sup>/K<sup>+</sup>-ATPase pump current was measured by two-electrode voltage clamp in Na<sup>+</sup>-loaded *Xenopus* oocytes expressing wild-type (WT), D801N or P775L variant human  $\alpha 3$  Na<sup>+</sup>/K<sup>+</sup>-ATPase. Pump currents were elicited by perfusing external solution containing 110 mM Na<sup>+</sup> and 5 mM K<sup>+</sup>. Currents specific to the exogenously expressed  $\alpha 3$ -Na<sup>+</sup>/K<sup>+</sup>-ATPase were isolated by subtracting measurements in 10 mM ouabain from measurements in 2  $\mu$ M ouabain, and values at 0 mV (the holding potential used) are shown.  $n = 10$  replicates for each construct; error bars = 95% CI; \*\*\* $P < 0.0001$  versus wild-type. (C) P775L introduces a negative leak current. Steady-state pump currents in 110 mM Na<sup>+</sup> and 5 mM K<sup>+</sup> were measured by ouabain subtraction of 100 ms pulses from 0 mV to the indicated voltages.  $n = 10$  replicates per construct; error bars = 95% CI. (D) The P775L leak current does not depend on extracellular K<sup>+</sup>. Steady-state pump currents in 115 mM Na<sup>+</sup> without K<sup>+</sup> were measured by ouabain subtractions in the same oocytes from C after wash-out of ouabain for 9 min. Fifty millisecond pulses from 0 mV to the indicated voltages were used due to cell death during long pulses to negative potentials.  $n = 10$ , error bars = 95% CI. (E) P775L variant  $\alpha 3$ -Na<sup>+</sup>/K<sup>+</sup>-ATPases reach the cell membrane. In two-electrode voltage clamp measurements, off-transient currents representing Na<sup>+</sup> movement out of its binding sites on  $\alpha 3$ -Na<sup>+</sup>/K<sup>+</sup>-ATPase were measured by ouabain subtraction in 115 mM Na<sup>+</sup> after 50 ms pulses from 0 mV to the indicated voltages. These currents were fitted to monoexponential decay functions and integrated over time, yielding the charge moved Q at each voltage.  $n = 10$ , error bars = 95% CI.

voltage; however, this was not the case for P775L, suggesting that voltage dependence was reduced.

### P775L $\alpha 3$ -Na<sup>+</sup>/K<sup>+</sup>-ATPase allows an inward leak of primarily Na<sup>+</sup>

Next, we investigated which ion species leak through P775L  $\alpha 3$ -Na<sup>+</sup>/K<sup>+</sup>-ATPase by varying extracellular cations and monitoring for changes in reversal potential. Since no known  $\alpha 3$ -Na<sup>+</sup>/K<sup>+</sup>-ATPase variants produce comparable leak currents, we used a disease variant of a different enzyme as a positive control:  $\alpha 1$ -Na<sup>+</sup>/K<sup>+</sup>-ATPase (ATP1A1) p.L104R, which conducts a mixed Na<sup>+</sup> and H<sup>+</sup> leak.<sup>20,21</sup>

To test for Na<sup>+</sup> leak, we replaced Na<sub>o</sub><sup>+</sup> (115 mM) with bulky cations, either N-methyl-D-glucamine (NMDG<sup>+</sup>) or trimethylammonium (TMA<sup>+</sup>) (Fig. 3A and B). Since oocytes vary in expression capacity, we performed paired measurements in each oocyte (Na<sup>+</sup>/NMDG<sup>+</sup> or Na<sup>+</sup>/TMA<sup>+</sup>) and normalized them to the current magnitude at –80 mV in Na<sup>+</sup> in that oocyte.<sup>21</sup> Neither normalization (Fig. 3B) nor the order of pairwise measurement (Supplementary Fig. 6A) affected the results. Removing Na<sub>o</sub><sup>+</sup> strongly shifted the reversal potential to the left, indicating that Na<sup>+</sup> was the primary ion driving P775L leak (Fig. 3B). L104R  $\alpha 1$ -Na<sup>+</sup>/K<sup>+</sup>-ATPase showed more modest shifts (Fig. 3B), suggesting that Na<sup>+</sup> made a greater relative contribution to P775L than L104R leak. This result was not an artifact of oocyte loading with Na<sub>o</sub><sup>+</sup>, as non-loaded oocytes produced the same results (Supplementary Fig. 6B).

To determine whether H<sup>+</sup> also contributed to P775L leak, we shifted the external pH from 7.6 to 6.6. Consistent with leakage of H<sup>+</sup>, this tenfold increase in [H<sup>+</sup>]<sub>o</sub> shifted the reversal potential to the right in the presence of Na<sub>o</sub><sup>+</sup> and K<sub>o</sub><sup>+</sup>, Na<sub>o</sub><sup>+</sup> alone and NMDG<sub>o</sub><sup>+</sup> (Fig. 3C). Interestingly, leak currents were non-linear at negative voltages and increased in the absence of Na<sub>o</sub><sup>+</sup> (Fig. 3A and C), reproducing the behaviour of ‘normal’ H<sup>+</sup> leaks through wild-type Na<sup>+</sup>/K<sup>+</sup>-ATPase.<sup>19</sup> However, we could not definitely rule out NMDG<sup>+</sup> leak under these non-physiological conditions, as oocytes could not be loaded with NMDG<sup>+</sup> (Supplementary Fig. 5B). The influence of H<sup>+</sup> on reversal potential was smaller for P775L than L104R  $\alpha 1$ -Na<sup>+</sup>/K<sup>+</sup>-ATPase (Fig. 3C). Taken together, these results indicate that P775L primarily causes an abnormal inward Na<sup>+</sup> leak under physiological conditions, likely accompanied by an inward H<sup>+</sup> leak (Fig. 3D).

### P775L impairs conformational changes during extracellular Na<sup>+</sup> binding

Finally, we investigated how P775L affects stepwise Na<sub>o</sub><sup>+</sup> binding at the enzyme’s three binding sites. Using cut-open vaseline gap voltage clamp, we measured the three sequential transitions between phosphorylated enzyme states with 0, 1, 2 or 3 bound Na<sup>+</sup> (Fig. 4A). Leak currents were inhibited under these conditions, allowing us to quantify Na<sub>o</sub><sup>+</sup>-mediated transient currents originating from movement of Na<sub>o</sub><sup>+</sup> into their binding sites. Transient currents consisted of three kinetic components, fast, medium and slow, corresponding to the different rates of the conformational changes during each binding/occlusion event.<sup>22</sup>

To isolate each kinetic component, we applied –190 mV voltage pulses of varying length up to 25 ms, reflecting the dynamics of the system moving from right to left in Fig. 4A. The negative voltage drove Na<sup>+</sup> binding, starting with the rightmost, fastest transition and proceeding leftwards at longer timescales. The resulting transient currents (Fig. 4B) allowed quantification of the amount of Na<sup>+</sup> bound at –190 mV by each of the three kinetic components

from the multiexponential function of charge recovery over time after return to 0 mV. P775L severely reduced the relative contribution of the slow component, i.e. the leftmost step in Fig. 4A, and slightly slowed the time constant of this state transition (Fig. 4C). The absolute amount of charge moved by the slow component also decreased (Fig. 4C). In contrast, both the medium and fast components showed relative increases in the charge moved and faster time constants. Therefore, at –190 mV, P775L impairs the dynamics of all components and shifts the distribution of the enzyme population toward states with 1 and 2 Na<sup>+</sup> bound.

## Discussion

We identify a novel and strong genotype-phenotype correlation at the ATP1A3 locus between ATP1A3:c.2324C>T; p.(P775L) and spasticity with DD/ID and demonstrate cation leak as a new molecular mechanism of  $\alpha 3$ -Na<sup>+</sup>/K<sup>+</sup>-ATPase-associated disease. The possibility of ATP1A3-related disease should be considered in patients with spasticity of unknown origin and DD/ID, especially if associated with episodic movement disorders, epilepsy, normal brain MRI, or other neurological deficits. ATP1A3 should thus be incorporated into the differential diagnosis of complex HSP and spastic CP. Our findings indicate that changes in ion transport parameters beyond enzymatic rate contribute to phenotypic variability in Na<sup>+</sup>/K<sup>+</sup>-ATPase disorders.

Spasticity was a consistent clinical feature in all patients with ATP1A3:p.(P775L). It initially manifested within the first few years of life in five patients (Patients 3, 5, 6, 8 and 9), during adolescence in two patients (Patients 1 and 4) and after a catastrophic deterioration in one patient (Patient 2). The pattern of spasticity and associated weakness was consistently symmetric and was frequently diplegic (7/9). Spasticity was often progressive leading to a stepwise or gradual decline in motor function (5/9). Although spasticity can be seen in patients with AHC, especially in its later stages,<sup>23</sup> its early onset and consistency in patients with ATP1A3:p.(P775L) is noteworthy. In contrast to AHC, dystonia was infrequent and identified only in a single patient who experienced catastrophic deterioration. As the clinical distinction between dystonia and spasticity can be challenging, additional case identification and deeper phenotyping will be helpful to further clarify this point.

It is important to note that, besides spasticity, our patients had other variable features including episodic movement disturbances, as seen in AHC, CAPOS and RECA (Patients 2 and 3) or in hemiplegic migraine (Patient 6) but did not meet diagnostic criteria for these conditions. Their overall p.(P775L)-associated phenotype fits toward the mild end of the ATP1A3-related disease spectrum. The more severe manifestations in Patient 2 are likely sequelae of hypoxic brain injury rather than direct effects of p.P775L on neuronal signalling. He was apparently healthy until a fever-associated episode of prolonged cyanosis and rigidity; although EEG was not available at the treating hospital to determine whether this was a seizure, it is highly suggestive of an ATP1A3-associated generalized weakness episode with respiratory failure. Subsequent brain MRI confirmed injury rather than malformation. As episodes of weakness in ATP1A3-related diseases such as AHC are highly variable, we suggest that the same situation occurred in our cohort and other genetic or environmental factors may have caused Patient 2 to have an episode progressing to respiratory failure whereas the other patients with episodic symptoms did not.

Inward cation leak through P775L-variant enzymes represents a new mechanism of ATP1A3 pathogenesis. Previously described

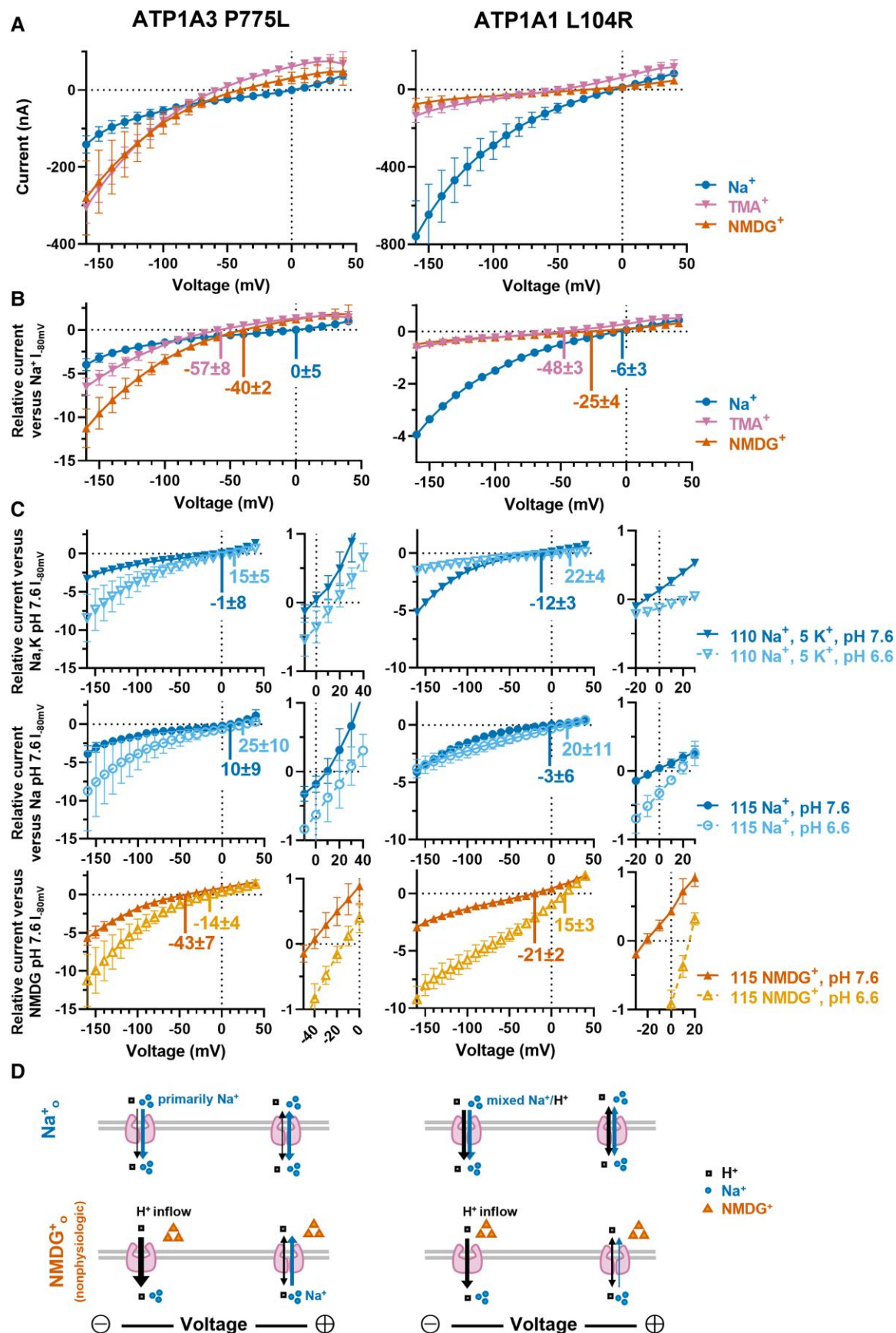
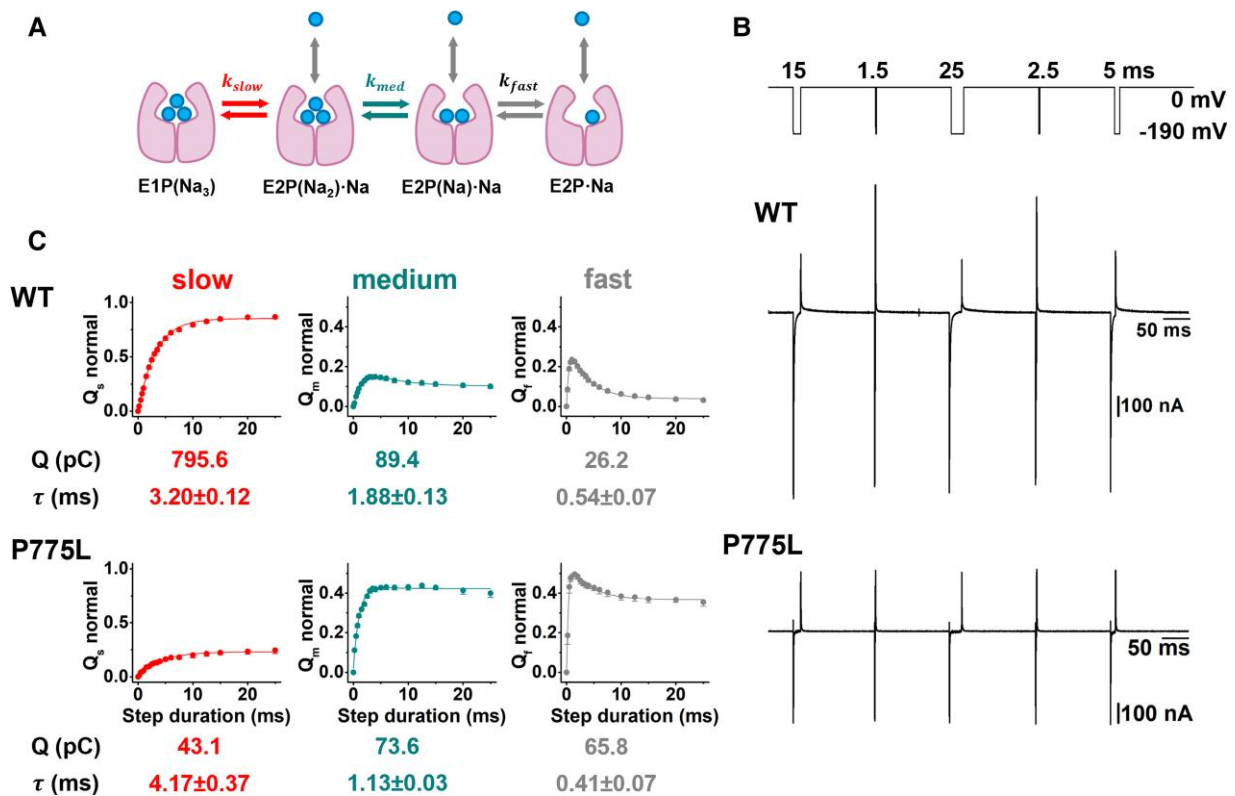


Figure 3 P775L leak current primarily involves inward movement of Na<sup>+</sup>, with a secondary H<sup>+</sup> component inhibited by extracellular Na<sup>+</sup>. *Xenopus* oocytes expressing P775L  $\alpha$ 3-Na<sup>+</sup>/K<sup>+</sup>-ATPase (ATP1A3 P775L; left) were compared to those expressing L104R  $\alpha$ 1-Na<sup>+</sup>/K<sup>+</sup>-ATPase (ATP1A1 L104R; right)

(continued)



**Figure 4** P775L disrupts the substrate ion binding sites, altering the kinetics of extracellular Na<sup>+</sup> binding. (A) Simplified schematic of the Na<sup>+</sup> binding/unbinding transitions studied. From right to left, three extracellular Na<sup>+</sup> sequentially bind to and occlude at the three sites within the enzyme, respectively producing fast ( $k_{fast}$ ), medium ( $k_{med}$ ) and slow ( $k_{slow}$ ) components of Na<sup>+</sup> on-transient currents. Applying negative voltage pulses as in B and C drives the enzyme state toward the left such that the first ion to bind represents the fast component. After the end of the pulse, Na<sup>+</sup> ions unbind from their binding sites, producing measurable off-transient currents. Therefore, the slow component represents the deocclusion and release of the first Na<sup>+</sup> to unbind when considered in the normal direction of the enzymatic cycle. (B) Na<sup>+</sup> transient currents are abnormal in P775L variant  $\alpha 3$ -Na<sup>+</sup>/K<sup>+</sup>-ATPases. Cut-open vaseline gap voltage clamp was done in *Xenopus* oocytes expressing P775L or wild-type (WT) ouabain-resistant  $\alpha 3$ -Na<sup>+</sup>/K<sup>+</sup>-ATPases. Every 40 s, 18 voltage pulses to −190 mV of various durations were applied, separated by 150 ms intervals. For clarity, five representative pulses with durations of 15, 1.5, 25, 2 and 10 ms are shown. (C) P775L reduces the contribution of the slow component to Na<sup>+</sup> transient currents. The amounts of charge moved by the slow ( $Q_s$ ), medium ( $Q_m$ ) and fast ( $Q_f$ ) components were normalized to the total amount of charge at the longest (25 ms) prepulse and plotted as a function of time. Solid lines represent exponential functions with  $\tau_s$ ,  $\tau_m$  and  $\tau_f$  fixed to the average values obtained from the independent fittings of each experiment. Below each plot, the non-normalized charge  $Q$  moved by each component and the time constant  $\tau$  calculated from the longest (25 ms) pulses are shown.  $n = 9$  for wild-type (WT) and  $n = 5$  for P775L.

pathogenic variants reduce the ion transport rate and/or activate the unfolded protein response.<sup>11,24</sup> Here, Na<sup>+</sup> influx through P775L-variant enzymes would directly oppose Na<sup>+</sup> export by wild-type Na<sup>+</sup>/K<sup>+</sup>-ATPases in the same heterozygous cell. Importantly,

P775L leak currents occur under physiological [Na<sup>+</sup>]<sub>o</sub> and [K<sup>+</sup>]<sub>o</sub>, suggesting that passive Na<sup>+</sup> inflow due to the presence of the variant enzyme would reduce the total Na<sup>+</sup> export rate. On the other hand, inward leak through the P775L enzyme is clearly too small

### Figure 3 (Continued)

in two-electrode voltage clamp current measurements with ouabain subtractions. Error bars representing the 95% CI are shown in all figures unless too small to be visible. (A) Removal of Na<sup>+</sup> results in a negative shift of the reversal potential of P775L and L104R leak currents. Leak currents were measured by ouabain subtraction in 115 mM Na<sup>+</sup>, 115 mM trimethylammonium (TMA<sup>+</sup>) or 115 mM N-methyl-D-glucamine (NMDG<sup>+</sup>) external solution. Pairwise measurements were done in order to compare currents in the same oocyte, using either Na<sup>+</sup> and TMA<sup>+</sup> or Na<sup>+</sup> and NMDG<sup>+</sup>; therefore, the plot shows pooled values for Na<sup>+</sup>. For P775L,  $n = 6$  for Na<sup>+</sup>/NMDG<sup>+</sup> and  $n = 8$  for Na<sup>+</sup>/TMA<sup>+</sup>; for L104R,  $n = 8$  for Na<sup>+</sup>/NMDG<sup>+</sup> and  $n = 8$  for Na<sup>+</sup>/TMA<sup>+</sup>. (B) Normalization of currents corrects for variability between oocytes. Current measurements from A were normalized by dividing all measurements in each oocyte by the magnitude of current in that oocyte at −80 mV in Na<sup>+</sup>. Reversal potentials  $\pm$  standard deviation in mV were  $0 \pm 5$  (Na<sup>+</sup>),  $-57 \pm 8$  (TMA<sup>+</sup>), and  $-40 \pm 2$  (NMDG<sup>+</sup>) for P775L and  $-6 \pm 3$  (Na<sup>+</sup>),  $-48 \pm 3$  (TMA<sup>+</sup>), and  $-25 \pm 4$  (NMDG<sup>+</sup>) for L104R. (C) Increasing the extracellular H<sup>+</sup> concentration results in a positive shift of the reversal potential of P775L and L104R leak currents. Ouabain-subtraction currents are shown for pairwise measurements in the same oocyte at pH 7.6 versus 6.6 in external solution containing 110 mM Na<sup>+</sup> and 5 mM K<sup>+</sup> (top), 115 mM Na<sup>+</sup> (middle) or 115 mM NMDG<sup>+</sup> (bottom). Currents were normalized to the magnitude of current at pH 7.6 at −80 mV in the same oocyte, i.e. the NMDG<sup>+</sup> curves were normalized to the value in NMDG<sup>+</sup> at pH 7.6, not Na<sup>+</sup> as in A. A magnified view is shown to the right of each plot to better illustrate the reversal potentials. Reversal potentials  $\pm$  standard deviation in mV were  $-0.8 \pm 8$  (Na<sup>+</sup>/K<sup>+</sup> pH 7.6),  $15 \pm 5$  (Na<sup>+</sup>/K<sup>+</sup> pH 6.6),  $-43 \pm 7$  (NMDG<sup>+</sup> pH 7.6) and  $-14 \pm 4$  (NMDG<sup>+</sup> pH 6.6) for P775L. They were  $-12 \pm 3$  (Na<sup>+</sup>/K<sup>+</sup> pH 7.6),  $22 \pm 4$  (Na<sup>+</sup>/K<sup>+</sup> pH 6.6),  $-21 \pm 2$  (NMDG<sup>+</sup> pH 7.6) and  $-15 \pm 1$  (NMDG<sup>+</sup> pH 6.6) for L104R.  $n = 6$  replicates for each combination of condition and variant. (D) Schematic of the ion flows indicated by the data from A–C. P775L conducts primarily Na<sup>+</sup> and some H<sup>+</sup> leak in the presence of extracellular Na<sup>+</sup>, while L104R conducts a mixed Na<sup>+</sup>/H<sup>+</sup> leak as previously demonstrated.

to cancel out wild-type  $\text{Na}^+/\text{K}^+$  transport (pump current) or to depolarize the membrane. At physiological voltages, P775L leak is up to one third the magnitude of wild-type pump current, respectively  $-33 \text{ nA}$  versus  $+85 \text{ nA}$  at  $-80 \text{ mV}$  and  $-21 \text{ nA}$  versus  $+103 \text{ nA}$  at  $-50 \text{ mV}$  (Fig. 2C). Normally, the membrane potential in human cells depends primarily on  $\text{K}^+$  permeability through  $\text{K}^+$  leak channels with a much smaller contribution from  $\text{Na}^+/\text{K}^+$  pump current. Here, the partial decrease in net  $\text{Na}^+/\text{K}^+$  pump current would be of even less consequence, making P775L unlikely to significantly interfere with maintenance of membrane potential. This leads to a model where P775L causes loss-of-function with a greater effect on intracellular  $[\text{Na}^+]_i$  than that of a null allele, i.e. a mild dominant-negative effect preferentially affecting  $\text{Na}^+$  export. Possible consequences might include impairment of not only  $\text{Na}^+$  clearance after action potentials, but also other transport processes coupled to the  $\text{Na}^+$  gradient such as removal of toxic intracellular  $\text{Ca}^{2+}$  by the  $\text{Na}^+/\text{Ca}^{2+}$  exchanger. The  $\text{H}^+$  leak component might also contribute to pathogenesis by acidifying the cytoplasm, but its significance is less clear. Although other ATP1A3 disease variants reduce  $\text{H}^+$  import rate, this was in the absence of  $\text{Na}^+$  and has never been shown to have a physiological or pathological consequence.<sup>25,26</sup>

What is the origin of the leak current? Pro775 is located one alpha-helical turn away from  $\text{Na}^+$ -binding site III, towards the extracellular side (Supplementary Fig. 7). Since we identified alterations in the conformational changes associated with occlusion-deocclusion transitions, we hypothesize that P775L disrupts function of the external gates. The internal and external gates are tightly coupled during normal  $\text{Na}^+/\text{K}^+$ -ATPase cycling. If this coupling is broken, then gates at both ends might sometimes be open simultaneously, leading to inwardly directed  $\text{Na}^+$  and  $\text{H}^+$  leak at negative potentials. It is unlikely that P775L enzymes act as non-selective open channels as reported with palytoxin poisoning, since millions of times more current would be expected.<sup>27</sup>

One limitation of this study is that since we characterized the variant  $\text{Na}^+/\text{K}^+$ -ATPase in a non-neuronal model system, we cannot conclusively determine whether ion leak contributes to pathogenesis separately from other effects such as haploinsufficiency. This question would be best answered through the identification of other ATP1A3 variants causing ion leaks, and by producing animal models or patient-derived iPSCs to compare the effects of p.P775L and true haploinsufficient/null variants in heterozygous neurons. It would also be important to understand the subcellular localization of the variant protein and confirm that it reaches the plasma membrane in neurons, as it does in the oocyte system, by immunofluorescence or protein tagging.

Support for the relevance of cation leak with ATP1A3 P775L, however, comes from comparison to heterozygous pathogenic cation leaks in other P-type ATPases such as ATP1A1 and ATP2A2, as well as to previously characterized ATP1A3 variants. In ATP1A1  $\alpha 1\text{-Na}^+/\text{K}^+$ -ATPase, somatic variants in aldosterone-producing adenoma and heterozygous germline variants in epilepsy-renal hypomagnesaemia cause similar  $\text{Na}^+$  and  $\text{H}^+$  leaks, evident in our data with ATP1A1 L104R from aldosterone-producing adenoma (Fig. 3).<sup>20,21,28</sup> We have also observed ion leaks with a published epilepsy-renal hypomagnesaemia ATP1A1 variant that are smaller than those of P775L (not shown). It is important to note that in ATP1A1-related disease, the main mechanism of pathogenesis is loss-of-function rather than cation leak: multiple ATP1A1 pathogenic variants do not display leaks, and haploinsufficiency in itself can raise  $[\text{Na}^+]_i$ . However, analogous to the model we propose for ATP1A3, the additional inward ion flow through leaky ATP1A1 enzymes has been suggested to contribute to pathogenesis by

exacerbating the rise in intracellular  $\text{Na}^+$  that needs to be cleared by wild-type enzymes expressed from the unaffected allele. Similarly, several disease variants in ATP2A2  $\text{Ca}^{2+}$ -ATPase cause  $\text{Ca}^{2+}$  leaks.<sup>29</sup>

$\text{Na}^+$  inflow could also help explain why our patients have a symptomatic disease phenotype that is generally on the mild end of the ATP1A3 disease spectrum. The mildest extreme of the spectrum may consist of protein-null alleles, as there are still no reported patients with nonsense, frameshift, or isolated ATP1A3 deletion variants. Mouse studies suggest this is more likely due to a mild or non-penetrant phenotype than to early lethality, given that heterozygous null *Atp1a3* mice have no spontaneous motor deficits whereas heterozygous mice carrying the ortholog of the D801N AHC variant exhibit spontaneous seizures and death. On the severe end of the spectrum, AHC-causing ATP1A3 variants that have been studied in detail, such as the recurrent p.D801N, E815K and G947R variants, exert strong dominant-negative effects: they reduce wild-type pump current in the same cell and cause membrane depolarization in heterozygous neurons.<sup>25,30</sup> Variants with additional toxic effects, activating the unfolded protein response, also cause severe disease.<sup>24</sup> Thus, a dominant-negative effect of P775L limited to reducing the net rate of  $\text{Na}^+$  export would fit between these two extremes. It would be more deleterious than the pure haploinsufficiency of a null allele, explaining our identification of nine unrelated probands with disease due to this single missense allele whereas no null variants have been found. It would also be milder than the disruption of  $\text{Na}^+$ ,  $\text{K}^+$  and membrane potential by the AHC variants, consistent with the difference in severity.

How might cation leak contribute to our patients' atypical and mild phenotypes? We hypothesize that the interaction of a variant's biophysical properties with the cellular environment influences which cell populations are most severely affected and therefore the localization of neurological deficits. For example, preferential impairment of  $\text{Na}^+$  export with P775L might most severely affect cells that frequently reach high  $[\text{Na}^+]_i$ , or are most sensitive to  $[\text{Na}^+]_i$ , perhaps including motor neurons where persistent influx through  $\text{Na}^+$  channels causes sustained firing in spasticity.<sup>31</sup> On the other hand, additional factors clearly influence severity, which varied within our cohort for features such as intellectual functioning and extent of motor involvement. Further studies examining correlations between 'atypical' phenotypes and molecular effects beyond enzyme activity could lead to better classification of disease variants based on genotype.

## Acknowledgements

This research was performed with the support of the NINDS Flow and Imaging Cytometry Core Facility (Dr Dragan Maric), National Institutes of Health (NIH). We would like to thank the families for participating in our study. This work was made possible by the generous gifts to Children's Mercy Research Institute and Genomic Answers for Kids program at Children's Mercy Kansas City.

## Funding

D.G.C. was supported by NIH Brain Disorders and Development Training Grant (T32 NS043124-19) and Muscular Dystrophy Association (MDA) grant 873841. J.R.L. was supported by US National Human Genome Research Institute (NHGRI) and National Heart Lung and Blood Institute grant to Baylor-Hopkins Center for Mendelian Genomics (UM1 HG006542), US NHGRI to

BCM-Genomics Research Elucidates the Genetics of Rare disease (GREGoR) (U01HG011758), US National Institute of Neurological Disorders and Stroke (R35NS105078) and MDA (512848). S.T.Y., C.M. and M.H. were supported by the National Institutes of Health (NIH Intramural Research Program).

## Competing interests

The authors report no competing interests.

## Supplementary material

[Supplementary material](#) is available at *Brain* online.

## Data availability

Data supporting the findings of this study are available from the corresponding author, upon reasonable request.

## References

- Clausen MV, Hilbers F, Poulsen H. The structure and function of the Na,K-ATPase isoforms in health and disease. *Front Physiol.* 2017;8:371.
- Jiao S, Johnson K, Moreno C, Yano S, Holmgren M. Comparative description of the mRNA expression profile of Na(+)/K(+)-ATPase isoforms in adult mouse nervous system. *J Comp Neurol.* 2022;530:627–647.
- de Carvalho Aguiar P, Sweadner KJ, Penniston JT, et al. Mutations in the Na<sup>+</sup>/K<sup>+</sup>-ATPase alpha3 gene ATP1A3 are associated with rapid-onset dystonia parkinsonism. *Neuron.* 2004;43:169–175.
- Rosewich H, Thiele H, Ohlenbusch A, et al. Heterozygous de-novo mutations in ATP1A3 in patients with alternating hemiplegia of childhood: a whole-exome sequencing gene-identification study. *Lancet Neurol.* 2012;11:764–773.
- Heinzen EL, Swoboda KJ, Hitomi Y, et al. De novo mutations in ATP1A3 cause alternating hemiplegia of childhood. *Nat Genet.* 2012;44:1030–1034.
- Sasaki M, Sumitomo N, Shimizu-Motohashi Y, et al. ATP1A3 Variants and slowly progressive cerebellar ataxia without paroxysmal or episodic symptoms in children. *Dev Med Child Neurol.* 2021;63:111–115.
- Miyatake S, Kato M, Kumamoto T, et al. De novo ATP1A3 variants cause polymicrogyria. *Sci Adv.* 2021;7(13):eabd2368.
- Vetro A, Nielsen HN, Holm R, et al. ATP1A2- And ATP1A3-associated early profound epileptic encephalopathy and polymicrogyria. *Brain.* 2021;144:1435–1450.
- Prange L, Pratt M, Herman K, et al. D-DEMO, a distinct phenotype caused by ATP1A3 mutations. *Neurol Genet.* 2020;6:e466.
- Demos MK, van Karnebeek CD, Ross CJ, et al. A novel recurrent mutation in ATP1A3 causes CAPOS syndrome. *Orphanet J Rare Dis.* 2014;9:15.
- Lazarov E, Hillebrand M, Schroder S, et al. Comparative analysis of alternating hemiplegia of childhood and rapid-onset dystonia-parkinsonism ATP1A3 mutations reveals functional deficits, which do not correlate with disease severity. *Neurobiol Dis.* 2020;143:105012.
- Kanai R, Ogawa H, Vilsen B, Cornelius F, Toyoshima C. Crystal structure of a Na<sup>+</sup>-bound Na<sup>+</sup>,K<sup>+</sup>-ATPase preceding the E1P state. *Nature.* 2013;502:201–206.
- Hubisz MJ, Pollard KS, Siepel A. PHAST And RPHAST: Phylogenetic analysis with space/time models. *Brief Bioinform.* 2011;12:41–51.
- Ioannidis NM, Rothstein JH, Pejaver V, et al. REVEL: an ensemble method for predicting the pathogenicity of rare missense variants. *Am J Hum Genet.* 2016;99:877–885.
- Rentzsch P, Schubach M, Shendure J, Kircher M. CADD-Splice-improving genome-wide variant effect prediction using deep learning-derived splice scores. *Genome Med.* 2021;13:31.
- Li XY, Hong YH, Wang L, Wan XH. Movement disorders rounds: atypical cases in two Chinese families with novel variants in ATP1A3. *Parkinsonism Relat Disord.* 2020;78:189–191.
- Mikati MA, Panagiotakaki E, Arzimanoglou A. Revision of the diagnostic criteria of alternating hemiplegia of childhood. *Eur J Paediatr Neurol.* 2021;32:A4–A5.
- Rosewich H, Sweney MT, DeBrosse S, et al. Research conference summary from the 2014 international task force on ATP1A3-related disorders. *Neurol Genet.* 2017;3:e139.
- Vedovato N, Gadsby DC. Route, mechanism, and implications of proton import during Na<sup>+</sup>/K<sup>+</sup> exchange by native Na<sup>+</sup>/K<sup>+</sup>-ATPase pumps. *J Gen Physiol.* 2014;143:449–464.
- Meyer DJ, Gatto C, Artigas P. On the effect of hyperaldosteronism-inducing mutations in Na/K pumps. *J Gen Physiol.* 2017;149:1009–1028.
- Azizan EA, Poulsen H, Tuluc P, et al. Somatic mutations in ATP1A1 and CACNA1D underlie a common subtype of adrenal hypertension. *Nat Genet.* 2013;45:1055–1060.
- Holmgren M, Wagg J, Bezanilla F, Rakowski RF, De Weer P, Gadsby DC. Three distinct and sequential steps in the release of sodium ions by the Na<sup>+</sup>/K<sup>+</sup>-ATPase. *Nature.* 2000;403:898–901.
- Mikati MA, Kramer U, Zupanc ML, Shanahan RJ. Alternating hemiplegia of childhood: clinical manifestations and long-term outcome. *Pediatr Neurol.* 2000;23:134–141.
- Arystarkhova E, Haq IU, Luebbert T, et al. Factors in the disease severity of ATP1A3 mutations: Impairment, misfolding, and allele competition. *Neurobiol Dis.* 2019;132:104577.
- Li M, Jazayeri D, Corry B, et al. A functional correlate of severity in alternating hemiplegia of childhood. *Neurobiol Dis.* 2015;77:88–93.
- Roenn CP, Li M, Schack VR, et al. Functional consequences of the CAPOS mutation E818 K of Na(+),K(+)-ATPase. *J Biol Chem.* 2019;294:269–280.
- Artigas P, Gadsby DC. Large diameter of palytoxin-induced Na/K pump channels and modulation of palytoxin interaction by Na/K pump ligands. *J Gen Physiol.* 2004;123:357–376.
- Schlingmann KP, Bandulik S, Mammen C, et al. Germline de novo mutations in ATP1A1 cause renal hypomagnesemia, refractory seizures, and intellectual disability. *Am J Hum Genet.* 2018;103:808–816.
- Kaneko M, Desai BS, Cook B. Ionic leakage underlies a gain-of-function effect of dominant disease mutations affecting diverse P-type ATPases. *Nat Genet.* 2014;46:144–151.
- Simmons CQ, Thompson CH, Cawthon BE, et al. Direct evidence of impaired neuronal Na/K-ATPase pump function in alternating hemiplegia of childhood. *Neurobiol Dis.* 2018;115:29–38.
- Li Y, Gorassini MA, Bennett DJ. Role of persistent sodium and calcium currents in motoneuron firing and spasticity in chronic spinal rats. *J Neurophysiol.* 2004;91:767–783.